IEEE Access
Multidisciplinary ⋮ Rapid Review ⋮ Open Access Journal

Received March 11, 2020, accepted April 7, 2020, date of publication April 15, 2020, date of current version April 30, 2020.

Digital Object Identifier 10.1109/ACCESS.2020.2988091

Generation and Diagnostics of Ambient Air Glow Discharge in Centimeter-Order Gaps

VLADISLAV GAMALEEV[1], TAKAYOSHI TSUTSUMI[1], MINEO HIRAMATSU[2], MASAFUMI ITO[2], (Member, IEEE), AND MASARU HORI[1], (Member, IEEE)

[1]Center for Low-Temperature Plasma Sciences, Nagoya University, Nagoya 468-8603, Japan
[2]Department of Electrical and Electronic Engineering, Meijo University, Nagoya 468-8502, Japan

Corresponding author: Vladislav Gamaleev (vlad@plasma.engg.nagoya-u.ac.jp)

This work was supported in part by the MEXT-Supported Program for the Strategic Research Foundation at Private Universities under Grant S1511021, in part by the JSPS KAKENHI under Grant 19H05462 and Grant 19H01889, and in part by the Plasma-bio consortium project under Grant 01221907.

ABSTRACT Re-pulsing glow discharges in gaps up to 2 cm were experimentally investigated in atmospheric pressure air. Discharge was ignited as a sequence of spark and glow discharge and sustained in a glow regime after ignition. It was confirmed that the discharge with defined parameters could be ignited without any adjustments after initiation of the discharge. The discharges were characterized by a high-speed camera, current and voltage measurements, and optical emission spectrometry (OES). Typical structure of the glow discharge consisting of cathode glow, dark faraday space, positive column, and anode glow was observed. Transition from subnormal to normal glow mode was confirmed by analysis of current and voltage waveforms. It was found by OES that the type of discharge strongly affects the ratio of produced reactive species. It was confirmed that with change of discharge from subnormal to normal glow regime, rotational temperature could vary across a wide range (from 1650 to 3500 K). The developed device allows glow discharge to be ignited with defined parameters, which makes the control of the gas temperature and ratio of reactive species possible by presetting the discharge parameters. Additionally, it was demonstrated that corona discharge or repeating spark discharges could also be generated using the developed device without additional manipulations of the experimental setup by adjusting the discharge parameters.

INDEX TERMS Glow discharge, gliding arc, OES, air plasma.

I. INTRODUCTION

Recently, atmospheric pressure plasmas are of great interest, owing to simple operation (not employing vacuum system), reduced processing cost, and the possibility of the application of plasma to samples which are not compatible with low-pressure conditions [1]–[5]. On the other hand, the fast development of non-equilibrium (also called non-thermal or cold) plasmas in the last two decades has allowed the application of plasma technologies in medicine and agriculture [3], [6]–[10]. In this case, the non-equilibrium nature of the plasma (temperature of electrons is much higher than temperature of gas) allows the creation of reactive species without excessive heat of the gas and treatment of targets which are sensitive to overheating (polymers, plants, tissues, etc.) [3], [7], [11]. A large number of possible applications results in the requirement of atmospheric pressure plasmas with various parameters, depending on applications.

One of the most well-studied non-equilibrium discharges is glow discharge [12]–[17]. However, it appears that maintaining low gas temperature of atmospheric pressure glow discharge is not an easy task [18]. The gas temperature of glow discharge is defined by the rate of energy transfer from electrons accelerated by electric field to the neutral gas and cooling of gas (molecules could leave the discharge area or transfer heat to electrodes). In the case of operation at low pressure, cooling could overcome heating, resulting in low temperature of the gas; however, cooling efficiency in the case of atmospheric pressure plasmas is decreased owing to the decrease of cooling surface at the same power compared to the low pressure [18]. Additionally, in the case of molecular gases, transfer of energy from electrons to molecules could be more effective, owing to additional energy modes of vibrational and rotational energy [13]–[15], [18].

The associate editor coordinating the review of this manuscript and approving it for publication was Jenny Mahoney.

Typically, electron temperature is comparable to the vibrational temperature of the molecule, resulting in effective electron energy transfer to the vibrational modes, with following transfer of energy from vibrational to rotational modes through relaxation [18]. As a result, the heating of molecular gases by atmospheric pressure plasmas is much higher compared to atomic gases. Higher temperatures of molecular gases result in significant limitations of use in biomedical, agricultural, and surface modification applications.

The use of noble gases (Ar or He), together with the flow of gas through the discharge area, allows to achieve low temperatures, which is a common approach in medicine and agriculture [3], [6]–[8]. Non-equilibrium atmospheric pressure plasma jets (NE APPJs) employing Ar or He as a process gas could be operated at temperatures below 37 °C, which is safe for the human body [19]–[21]. In this case, dielectric barrier discharge (DBD) plasma could be directly exposed to the target (wound, plant, seed, etc.), resulting in the application of electric field, UV radiation, and reactive species produced by plasma. It was reported that reactive oxygen and nitrogen species (RONS) are important for the positive effects observed after plasma treatment (bactericidal effect, blood vessel relaxation, wound healing, selective killing of cancer cells, etc.) [22], [22]–[26].

However, the use of noble gases increases the cost of the treatment. Moreover, Ar or He DBD plasmas are not effective for the production of RONS, because the RONS are mostly generated by dissociation of molecules from air (N_2, O_2, and H_2O), which enter the discharge area from the surrounding gas [21], [27], [28]. The most cost-effective way to produce RONS is via the use of air as a process gas, owing to presence of the oxygen and nitrogen required for generation of RONS and low cost; however, the use of air typically results in elevated temperatures of the gas (above 2000 K), making application in medicine, agriculture, and various sorts of surface treatments (e.g., treatment of polymers) impossible [18], [27], [29].

A common approach to overcome the problem of excessive heat of molecular gases in atmospheric pressure plasmas is the treatment of gas flow and exposure of effluent to the target, avoiding contact with plasma. If gas flow and distance from the target are well tuned, it is possible to achieve low temperature of the effluent (even below 37 °C) and high concentration of reactive species delivered to the target, which allows low temperature processing [27], [30]–[32].

An additional problem is the scaling of the discharge for the treatment of a large amount of gas. Typically, for initiation of the discharge in air, about 10 kV per centimeter of the discharge gap length is required, which results in a bulky power supply in the case of gaps of a few centimeters. Commonly used approach to scale up the glow discharge in air is initiation of the discharge between electrodes with a smaller gap and the following extension of the gap length to desired value [12], [18]. Another approach is the use of an additional high frequency discharge system (breakdown voltage is lower in the case of high frequency systems) or hollow cathode discharge for initiation of the glow discharge [33]. In the case of the extension of the gap, the main disadvantage is the necessity of the use of a manipulator, when in the case of the use of high frequency discharge pre-ignition, it is necessary to use an additional power supply, which makes discharge setup more complex and costly.

A possible approach to increase the gap without a manipulator is the use of electrodes with extending length of gap, as shown in Figure 1.

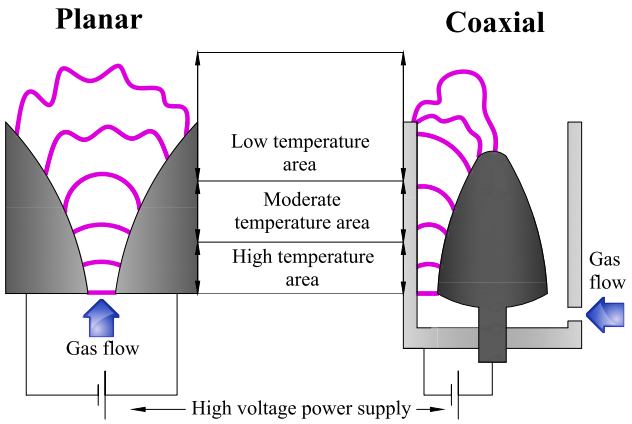

FIGURE 1. Schematic of planar gliding glow discharge (left) and rotating coaxial gliding glow discharge (right).

A planar knife-shaped electrode structure (Figure 1, left) allows to initiate the discharge at the place with a smaller discharge gap (lower area, typically gap length below 1 cm), and to extend discharge by the airflow to the region with a longer gap (upper area, gap length up to 10 cm depending on used power supply) [34], [35]. In this case, discharge will be initiated at a high temperature (above 3000 K) in a normal glow, abnormal glow, or arc mode, depending on input power and discharge conditions, and transferred to strongly non-equilibrium state (subnormal glow discharge) with extension of the gap between the electrodes. The extension of the gap results in a decrease of the discharge current with an increase of voltage and reduction of the gas temperature, resulting in moderate (2000–3000 K) or low (below 2000 K) temperature of the gas in the upper part of the discharge (Figure 1, left). When discharge is extended to the maximal length that can be sustained by the power supply, the discharge will be terminated and restarted at the area with the shortest discharge gap. In the literature, this type of discharge is commonly called "gliding arc" discharge. The term "gliding arc" was suggested based on the visual appearance of the discharge; however, the study of current and voltage characteristics, the structure of the discharge, and optical emission spectra suggests that the discharge burns in a glow regime rather than arc [36]–[38]. Therefore, in the present work, the authors use the term "gliding glow" discharge instead of "gliding arc."

Another approach to treat large volumes of gas is the use of coaxial electrodes, as shown in Figure 1 (right). In this

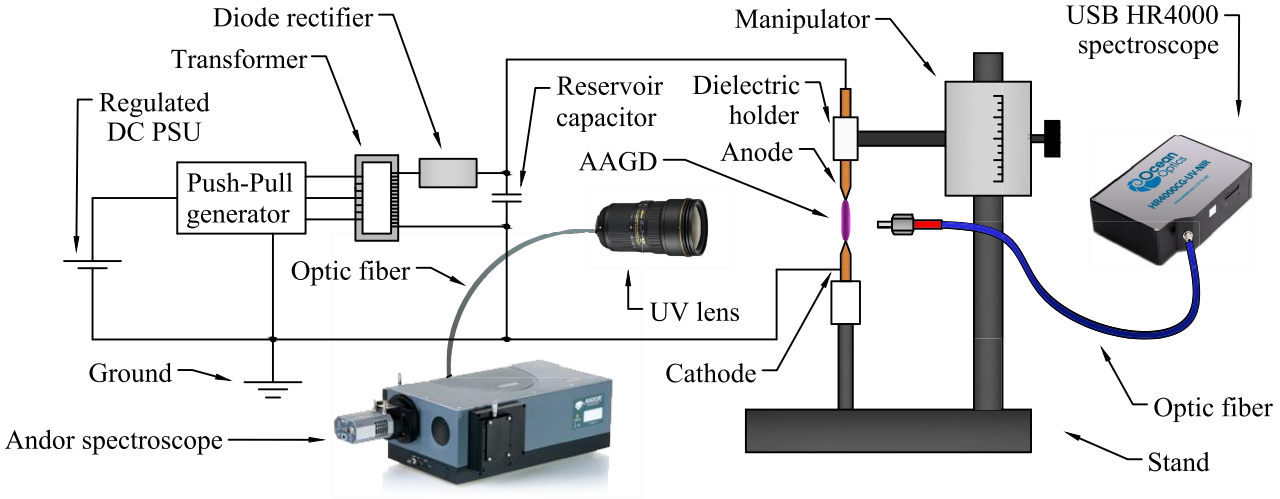

FIGURE 2. Experimental setup.

case, discharge is also initiated at the place with the shortest discharge gap and extended by the flow of gas. Additionally, rotation of the discharge could be achieved by the use of tangential gas flow, ensuring the effective treatment of large volumes of gases [29], [39], [40].

Gliding glow discharges are widely used in gas conversion, medicine, agriculture, and other studies; however, gliding glow discharge has a number of significant disadvantages. Firstly, in most applications, some range of plasma parameters is required for effective treatment, and typically, it is in subnormal glow regime (low temperature area on Figure 1), when another part of the plasma in a higher temperature region is not required or vice versa [34]. The changing of plasma parameters across a wide range when the desired point of interest is a small part of it results in ineffective electric power use. Additionally, the presence of plasma with undesired parameters could result in the production of unwanted reactive species, which could limit the application. Another drawback is the constantly changing plasma impedance, which results in problems with load matching and large values of reflected power. On the other hand, the constant change of current and voltage and the restrike of the discharge results in the presence of significant electromagnetic (EMI) noise during operation.

The perfect solution will be the initiation of the discharge in the larger gaps at desired parameters, avoiding elongation of the discharge. In this work, we demonstrate generation of the glow discharge at defined conditions in a centimeter-order gap (up to 2 cm) using a single power supply, which does not require any adjustments after the start of the discharge.

II. EXPERIMENTAL SETUP

In the present work, re-pulsing glow discharge was generated between two copper rod electrodes (99.5% Cu, CU-112544, Nilaco, Japan) by supplying high voltage to the upper electrode (anode) when the lower electrode (cathode) was electrically grounded. High voltage was supplied using a custom power supply consisting of a push–pull generator powered by a regulated direct current power supply (DC PSU), a high voltage transformer, a diode rectifier, and a reservoir capacitor. A schematic of the experimental setup is presented in Figure 2.

A self-oscillating push–pull generator, which is a modified version of the Royer converter, was used for the generation of a sinusoidal signal, which was fed to the primary of the transformer [41], [42]. The push–pull generator provides high efficiency (up to 90%) and features small parts count, which are essential for the development of a low-cost power supply. Power consumed by the push–pull generator is varied by the current and voltage set on the DC PSU. High voltage sinusoidal signal on the secondary winding of the transformer is rectified by a high voltage diode rectifier and supplied to the reservoir capacitor, resulting in the charging of the capacitor during positive half cycles and in the increasing of the output voltage by up to 25 kV. One significant drawback of the push–pull generator is the frequency shift caused by variation of the load (plasma impedance); however, despite frequency shift, the efficiency remains high and the frequency shift does not have a significant effect on the plasma parameters.

In the present work, the gap between the electrodes was adjusted using a manipulator prior to the generation of the discharge, and was kept the same during diagnostics of the discharge. To avoid disturbance of the discharge caused by external airflow, the entire discharge setup was placed in an airtight chamber.

Optical emission spectra of the discharge were recorded using a broad range optical emission spectroscope (HR4000CG-UV-NIR, Ocean optics) and a high-resolution spectroscope (Shamrock 500 monochromator with iStar DH734-18U-03 ICCD camera, Andor; optical resolution of 0.045 or 0.15 nm depending on used grating) with a lens (PF10545MF-UV, Nikon). The wavelength of the spectroscopes was accurately adjusted using a Hg reference lamp. Images of the plasma were recorded using a conventional

camera (D5100, Nikon) and a high-speed camera (Phantom v1610, Vision Research).

III. RESULTS AND DISCUSSION

A. GENERATION OF THE DISCHARGE

The power supply used in the present work allows to generate corona discharge, repeating spark discharges with corona discharge and re-pulsing glow-like discharge between two metal electrodes with spacing up to 2 cm. The discharge is generated in a same way as was reported elsewhere for the pin-to-liquid electrode setup, with sub-centimeter spacing between the electrode and surface of the liquid [25], [38]. The type of the discharge depends on the parameters set on the DC PSU.

In the case that there is no current passing through the load of the generator or the value of current is small (a few μA), it works as a DC high voltage power supply. To demonstrate performance of developed generator at low current mode, current supplied from DC PSU to the push–pull generator in the primary winding was limited by 1 A and voltage set on DC PSU was varied in a range from 5 to 25 V. In that case the reservoir capacitor is charged by rectified sunusoidal signal from the push–pull generator to the voltage defined by the turn ratio of the transformer and the voltage set on the DC PSU. After reaching maximum value, the voltage remains at the same level; however, some AC ripple with an amplitude dependent on load current could be observed in the voltage, because a low pass filter was not employed in the present work. If the voltage produced by the generator is sufficient, then positive corona could be observed. An example of current and voltage waveforms of corona discharge generated using current limited by 1 A and voltage set on DC PSU of about 23 V is presented in the Figure 3a. Corona discharge intensity and volume depends on voltage, and could change from a barely visible point (at voltage between the electrodes of about 15 kV) to a diffuse mode (at voltage between the electrodes of about 22 kV) that fills the entire volume between the electrodes (Figure 3b) similarly to diffuse corona discharge reported elsewhere [43].

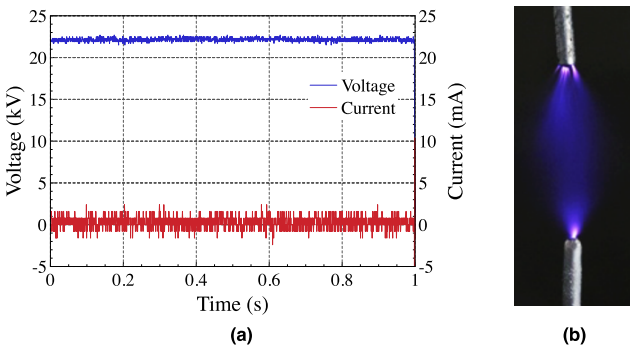

FIGURE 3. Current and voltage waveforms (a) and photo of corona discharge generated between two Cu rod electrodes with 2 cm spacing.

With further increase of voltage set on DC PSU (using the same limitation of current by 1 A) corona discharge will transfer to the transient spark discharge if the voltage between the electrodes is sufficient, in the same way as it was reported elsewhere [44]–[46]. Current and voltage waveforms of repeating spark discharges generated using current limited by 1 A and voltage set on DC PSU of about 25 V are presented in Figure 4a.

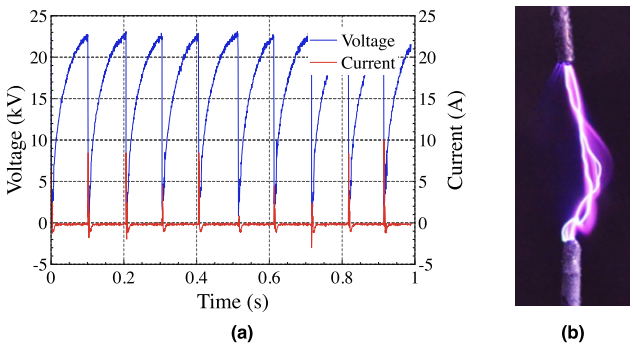

FIGURE 4. Current and voltage waveforms of repeating spark discharges (a) and photo of spark discharge (b) generated between two Cu rod electrodes with 2 cm spacing.

If the spark discharge is initiated, then the high conductivity of the spark plasma leads to a fast increase of current and a rapid drop in the voltage on the reservoir capacitor due to loss of charge. After termination of the spark discharge, the voltage on the capacitor starts to increase because of the current supplied from the transformer during positive half cycles of rectified sinusoidal signal. After the increase of voltage to the threshold value, firstly, corona discharge will appear, and at the moment when the voltage on the capacitor reaches breakdown voltage, the corona discharge will transfer to the spark. Both the corona discharge and the spark discharge are visible in the photo (Figure 4b), owing to the long exposure time of the camera. In this regime, repeating spark discharges could be observed. Breakdown voltage depends on the gap between the electrodes and gas filling the discharge gap. In the present work, the discharge generated in ambient air with a gap between the electrodes of 2 cm resulted in a breakdown voltage of about 22.5 kV. The frequency of the spark discharges could be controlled by the current set on the DC PSU. An increase of current supplied to the push–pull generator will result in faster charge of the reservoir capacitor and faster reaching of the breakdown voltage, leading to an increase in the frequency of spark discharges.

However, if the current supplied to the primary winding of the transformer is high enough (above 2.5 A for the present setup with 2 cm discharge gap) to provide current in the order of a few mA on the secondary winding, some continious discharge could be generated after the spark. Current and voltage waveforms and photos of such a discharge with variation of the current and voltage supplied to the push–pull generator are presented in Figure 5: current and voltage waveforms and photos of the re-pulsing discharge generated at a DC current of 3 A and a voltage of 8.5 V (a,b); current of 3.9 A and voltage of 8.5 V (c,d); current of 5 A and voltage of 11.5 V

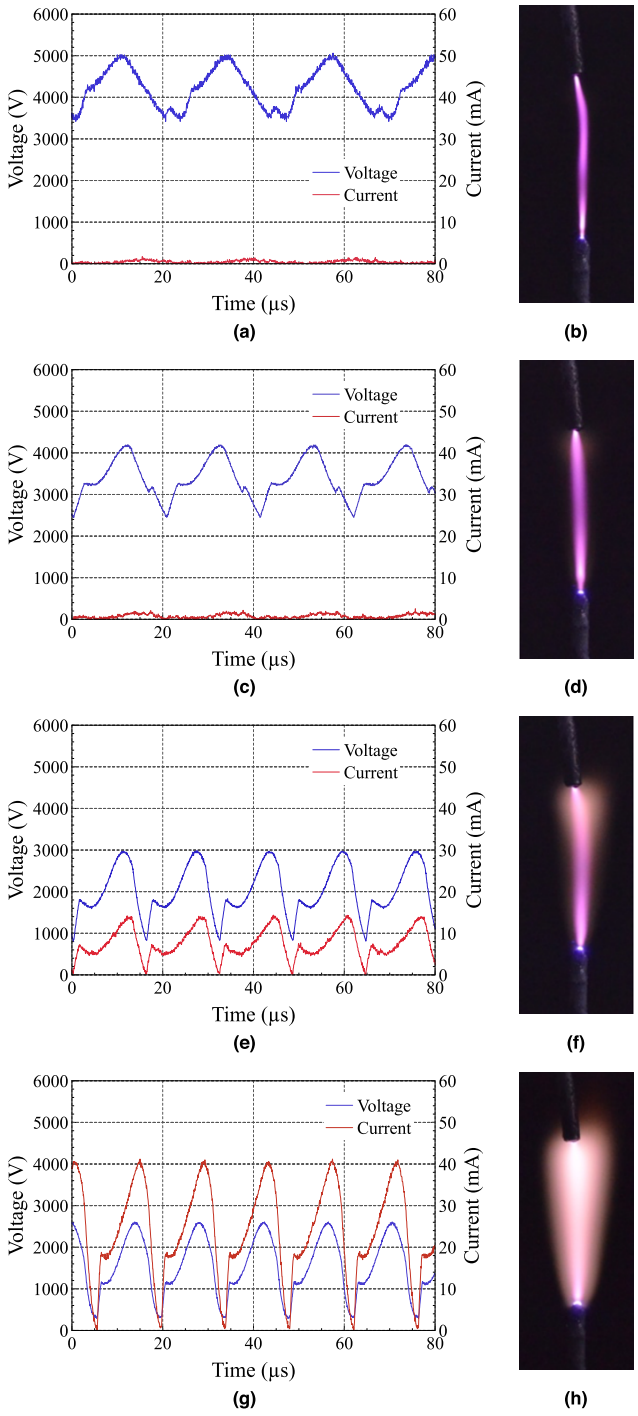

FIGURE 5. Current and voltage waveforms and pictures of re-pulsing discharges generated between two Cu rod electrodes with 2 cm spacing at currents supplied by DC PSU of 3 A (a,b), 3.9 A (c,d), 5 A (e,f), and 5.5 A (h,g), respectively.

(e,f); and current of 5.5 A and voltage of 15 V (g,h) supplied to the push–pull generator by the DC PSU.

It could be observed that continious discharge actually re-pulses with pulsation rate related to the frequency of oscillation produced by the push–pull generator. The current and voltage waveforms of each pulse are complex and depend on the conditions. The observed pulsation occurs during cyclic variation of charging and discharging of the reservoir capacitor during half cycles of rectified sinusoidal signal. Continious changes in charge accumulated in the reservoir capacitor and impedance of plasma, together with the ripple caused by switching of the push–pull generator, result in complex shapes of each discharge pulse (Figure 1S, supplementary data).

When plasma is stabilized, re-pulsing happens reproducibly if there are no external factors (e.g., external airflow) that can interfere with plasma. Depending on input power supplied to the push–pull generator, the current and voltage waveforms change.

With an increase of power, the current of the discharge increases and the voltage decreases (Figure 5a,c,e,g), and intensity of the optical emission and volume of the plasma also increase with an increase of power (Figure 5b,d,f,h). Despite changes in the shape of the current and voltage waveforms, it could be noted that for all presented conditions, plasma discharge pulse is generated when the voltage is above some threshold value and discharge is terminated when the voltage is below the thresold.

B. RELATION OF CURRENT AND VOLTAGE DURING THE DISCHARGE

It was observed in Figure 5 that with an increase of the discharge current, the voltage supplied to the electrodes is decreasing. Observed feature is typical for the transition from subnormal to normal glow discharge (Figure 2S, supplementary data). In the case of DC glow discharge current and voltage are constant; however, in the present work current and voltage waveforms of re-pulsing glow-like discharge are complex and maximal values of current and voltage diring the pulse of the discharge are not clearly representing feature of the discharge. Therefore, average values of current and voltage during large number of pulses were analyzed to investigate relation of current and voltage.

Average values of voltage as a function of the average discharge current for the discharges generated in a wide range of power supplied to the push-pull generator and gaps from 0.5 cm to 2 cm are summarized in the Figure 6.

Points on the curve for discharge gap of 2 cm on the Figure 6 when values of current are 0.74, 1.24, 2.98 and 16.9 mA are corresponding to conditions represented on the Figure 5(a), Figure 5(c), Figure 5(e) and Figure 5(g) respectively.

For the 2 cm gap between the electrodes average voltage is dropping rapidly from about 4300 V to 2400 V with increase of average current from 0.74 to 2.98 mA, when further increase of current to 8 mA results in decrease of voltage from 2400 V to only 2100 V. Further increase of current does not result in such a drop of voltage as it was observed in the case of average current below 3 mA. It could be concluded that re-pulsing discharge is behaving like subnormal glow discharge in the case of average currents below 3 mA, after that having some transition from subnormal to normal glow

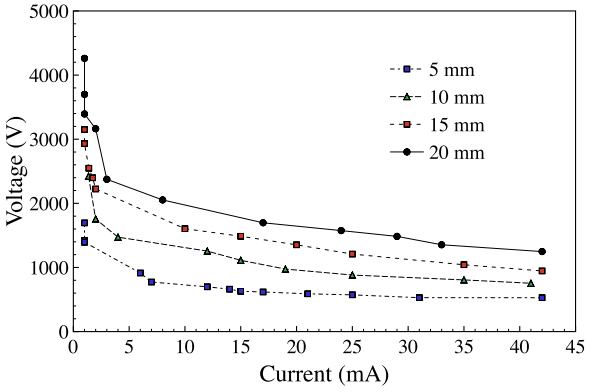

FIGURE 6. Average voltage applied to the electrodes as a function of the average discharge current with varied length of the discharge gap.

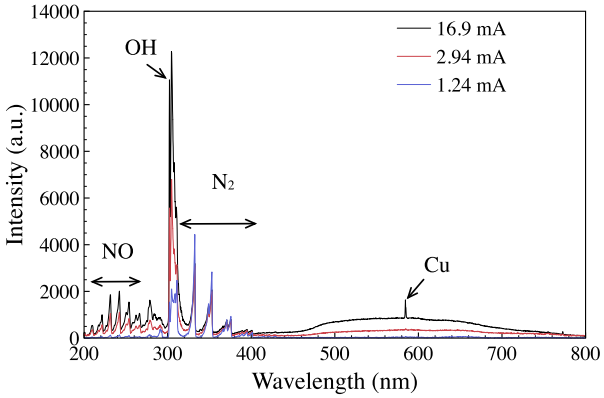

FIGURE 7. Optical emission spectra of the discharges generated in 2 cm gap with varied discharge current.

discharge state (hereafter "transitional glow") at currents between 3 and 8 mA and transfers to a normal glow regime at higher currents. Discharge at the average current of about 45 mA was maximal achiavable by the generator used in the present work.

In the case of smaller discharge gaps discharge behavior is the same. Average voltage drops rapidly with increase of average current of up to about 3 mA, and with a further increase of current up to 10 mA, there is some transitional area with moderate voltage drop, and voltage starts to decrease at a slower rate and becomes constant (which is clearly observed on the curve for a 0.5 cm gap), indicating that the discharge is transferring from a subnormal to a normal glow-like regime. Only one difference is observed with a decrease of the gap length between the electrodes, which is the decrease of average voltage for the similar values of average current, which is related to a decrease of the threshold voltage for initiation of the discharge.

C. OVERVIEW OPTICAL EMISSION SPECTRA

Another characteristic important for understanding the type of discharge is the optical emission spectra. Emission spectra of the discharge in a wide range of wavelength was recorded using the Ocean Optics HR4000 optical emission spectroscope with quartz optic fiber. Optic fiber was placed at a distance of 3 cm from the discharge (so as not to interfere with the discharge) in the middle of the discharge gap. The recorded optical emission spectra for subnormal glow-like discharge (1.24 mA), transitional glow discharge (2.94 mA), and normal glow-like discharge (16.9 mA) are depicted in Figure 7.

The dominant emission lines observed in the spectra are OH emission lines at 307 and 309 nm, N_2 second positive emission bands at 337, 358, and 382 nm, and NO γ bands in the wavelength range of 220–290 nm. Despite the strong emission of the OH originated from the dissociation of water molecules presented in the air, emission lines of hydrogen (486 nm H_α and 656 nm H_β) were not observed in the spectra.

The authors do not have a clear explanation for the broad continious emission observed in the region between 450 and 800 nm for discharges with currents of 2.94 and 16.9 mA. Considering that this continuum emission was not observed in the case of 1.24 mA discharge, it could be concluded that it comes from the white area of the plasma (Figure 4f,h), which does not appear in the case of low current (Figure 4b,d). Taking into account the higher power of the discharge, white continuum emission could be attributed to the overlapping of abundant energy levels for the diatomic molecule (N_2 (B-A)) and black body radiation [16], [47], [48].

The other difference which is observed with variation of the discharge current is the ratio of OH and N_2 emission intensity. An increase of current results in a significant increase of OH emission intensity when N_2 emission intensity decreases.

All other emission lines (except the peak for Cu at 593 nm observed in the case of current of 16.9 mA) remained in a similar ratio with change of the discharge current.

The presence of a second positive system of N_2 in the emission spectra and the dependance of the voltage on the discharge current discussed above suggests that the re-pulsing discharge observed in the present work burns in a subnormal or normal glow regime.

D. HIGH-SPEED CAMERA IMAGING

The other indication of the glow regime of the discharge is the structure of the plasma column. Figure 8 illustrates images of the discharge obtained with various exposure times of the camera. No image was recorded from the subnormal glow discharge at 300 and 700 μs exposure time (Figure 8a,b, respectively), owing to the low intensity of the optical emission.

It could be observed that, irrespectively of discharge current, the structure of the discharge is similar. There are two bright areas in the area of the electrodes which could be observed in the plasma, even at a short exposure time, when the bulk of the plasma is not visible (Figure 8c,f,i). Additionally, emission on the bottom electrode (cathode) could be observed in Figure 8e when emission from the top electrode (anode) is barely visible, indicating that the intensity of

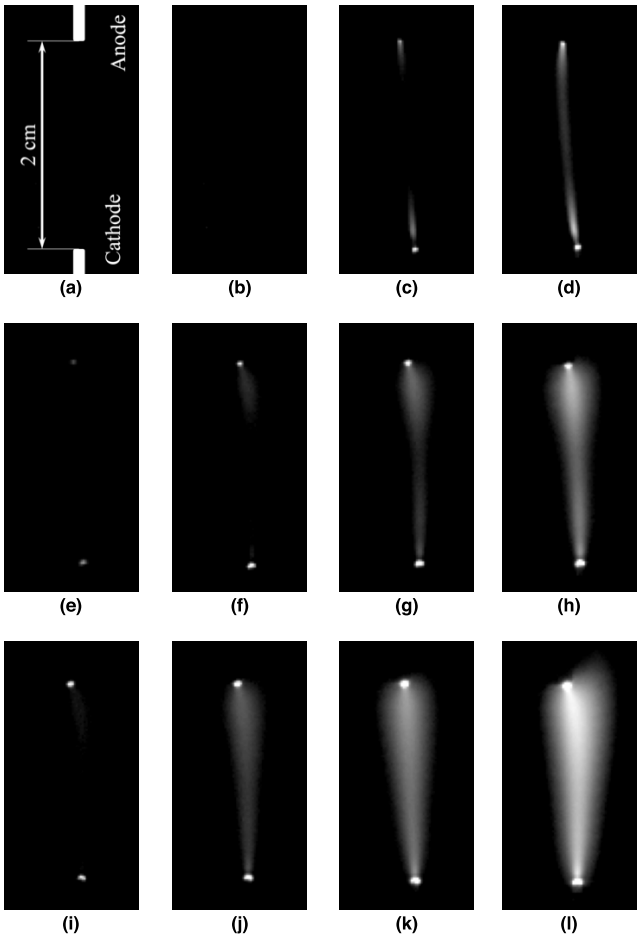

FIGURE 8. Images of the plasma at a current of 1.24 mA (a–d), 2.94 mA (e–h), and 16.9 mA (i–l), recorded with an exposure time of 100 μs (a,e,i), 300 μs (b,f,j), 700 μs (c,g,k), and 1900 μs (d,h,l).

the emission from the cathode area is higher compared to the anode area.

With an increase of the exposure time, the bulk of the plasma could be visualized. In all of the cases, some small dark spaces between cathode emission and the plasma bulk are clearly visible (Figure 8c,d,g,h,j–l). It could be concluded that the emission consists of a strong cathode emission, dark space, plasma bulk, and anode emission, which is the same as the structure of the glow discharge (cathode glow, dark Faraday space, positive column, and anode glow) [13]–[15], [18], [49].

It could be concluded that re-pulsing discharge has the structure of the glow discharge, featuring cathode glow, dark Faraday space, positive column, and anode glow. Considering the dependency of the voltage on the discharge current, the presence of a second positive system of N_2, and the structure of the discharge, it could be stated that the discharge studied in the present work burns in subnormal or normal glow regime, depending on the discharge parameters.

In the case of the higher currents (2.94 and 16.9 mA), firstly, the center of the positive column was visualized

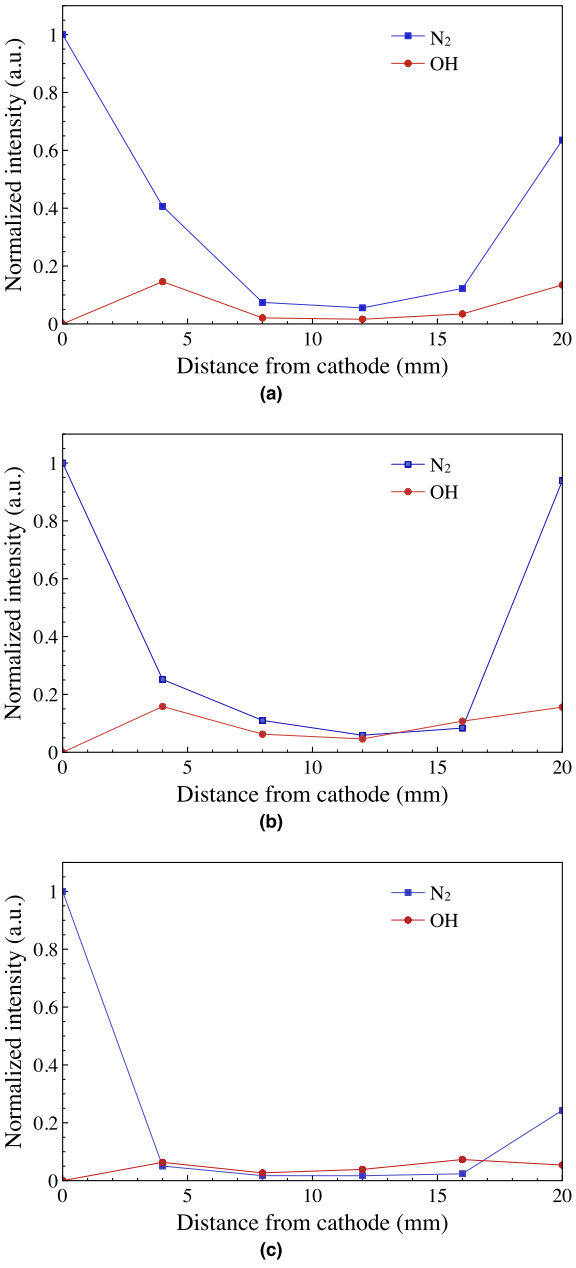

FIGURE 9. Spatially resolved normalized intensities of OH and N_2 prominent emission lines for discharges at currents of 1.24 mA (a), 2.94 mA (b), and 16.9 mA (c).

(Figure 8g,j) when the white emission surrounding the plasma core was visualized only at longer exposure times (Figure 8h,k,l), indicating that the white emission (possibly responsible for the continuum emission in the region 450–800 nm) has lower intensity compared to the plasma core.

E. EFFECT OF THE DISCHARGE PARAMETERS ON THE INTENSITY OF OH AND N_2 OPTICAL EMISSION

In the overview spectra the highest differences were observed for N_2 and OH emission bands. To analyze the effect of the

conditions on the OH and N_2 emission ratio, optical emission spectra were recorded in a region between 300 and 345 nm (Figure 3S, Supplementary data) using a high-resolution spectroscope (optical resolution of 0.15 nm), and the intensity of the prominent peaks (309 nm for OH and 337 nm for N_2) were compared. The recorded emission intensity was normalized to the emission of N_2 in the cathode area. Spatially resolved normalized intensities of OH and N_2 prominent emission lines for the discharges at various currents are presented in Figure 9.

It could be observed that for all discharge currents, emission from OH in the cathode area is neglible and most of the emission comes from the N_2. Additionally, in all of the cases, emission intensity at the cathode area is stronger than that in the anode area, which correlates well with the observation by high-speed camera and the type of discharge discussed above. Intensity of both OH and N_2 decreases in the center of the gap, which also correlates with the weaker intensity observed in the central area by the high-speed camera.

For the discharge in the subnormal glow regime (Figure 9a), the intensity of the OH is much lower than the intensity of N_2 in the entire discharge gap, indicating a small amount of OH radicals. Meanwhile, in the case of transitional glow (Figure 9b), the level of OH emission is higher compared to subnormal glow; moreover, the normalized intensity of the OH emission is higher than that of N_2 in the top area of the positive column.

From the photo (Figure 5f), it could be noted that the area of high OH intensity is the area where white emission around the core plasma could be observed. In the case of normal glow discharge (Figure 9c), the normalized intensity of the OH emission is higher compared to the subnormal and transitional glow regimes; also in the positive column, the intensity of OH is higher than that of N_2 in the entire area of observation. In the case of normal glow discharge, the entire positive column featured white emission with stronger intensity in the anode area (Figure 5h), which clearly correlates with the spatially resolved normalized intensity of the OH emission line (Figure 9c).

The increase of OH emission could be explained by an increase of electron excitation energy with an increase of the power supplied to the plasma. The excited states of OH are mostly produced by dissociative excitation of water molecules (threshold 18.5 eV), when the N_2 excited state responsible for emission around 337 nm is produced by direct excitation with lower energy (threshold 11.18 eV). The presence of mostly N_2 emissions in the case of subnormal glow indicates that the energy of the electrons is not enough for dissociative excitation of water, when in the transitional glow, the energy of the electrons in the upper part of the positive column increases above the threshold of 18.5 eV, and in the case of normal glow discharge in the entire positive column, there are enough electrons with energies higher than 18.5 eV for dissociative excitation.

It could also be concluded that the area with white emission observed for transitional and normal glow discharge features some electrons with relatively high energy (above 18.5 eV) for the production of a larger amount of OH.

F. ESTIMATION OF ROTATIONAL TEMPERATURE

Another important parameter for understanding the plasma discharge process and for possible practical applications is the temperature of the gas. In the case of non-equilibrium atmospheric pressure plasma, rotational temperature is close to translational (gas) temperature due to frequent collisions among heavy particles [18], [50], [51]; therefore, rotational temperature will represent the same dependency on the discharge parameters and could be used as an estimate for the gas temperature.

Estimation of the rotational temperature of N_2 was done by comparison of the measured N_2 emission band to the simulation. In the present work rotational emission band from the second positive system of N_2 ($C^3\Pi_u(v' = 0) \rightarrow B^3\Pi_g$ ($v'' = 0$)) with bandhead at 380.5 nm was used. As discussed above, gas tempertaure has been assumed equal to rotational tempertaure of nitrogen in the N_2 (C(v'=0)) state.

In order to get rotational tempertaure, the mentioned emission band was calculated using the optical constants reported by Herzberg [52] and convoluted with the actual resolution of the used monochromator, in a similar way as it was reported elsewhere [50], [53], [54]. The spectra calculation procedure included three steps: the calculation of the rotational line positions in each of bands, application of the line intensity factors (Honl-London factors) and numerical convolution of the obtained spectrum with the intrumental function of the monochromator. Spectra were simulated in the range of rotational temperatures from 300 K to 5000 K with step of 20 K. The temperature was determined from the best match (using least square method and manual matching) of simulated spectra and measured experimental spectrum.

An example of the measured (optical resolution of 0.045 nm) and simulated spectrum is presented in Figure 4S (supplementary data). The measurement of spectra suitable for reliable matching to the simulated spectrum required a large integration time to reduce noise (owing to low emission intensity in the area of 380.5 nm). In the case of subnormal discharge at low current (0.74 mA), the discharge was fluctuating, resulting in distortion of the measured emission spectrum. In the case of normal glow discharge, long accumulation of the signal was not possible, owing to the heating and melting of electrodes during accumulation time. Therefore, rotational temperatures were estimated for subnormal glow (1.24 mA) and transitional glow (2.94 mA) discharges. Figure 10 represents the spatially resolved rotational temperatures on N_2 for subnormal and transitional glow discharges.

It could be noted that rotational temperature is lower in the cathode and anode areas for both subnormal and transitional glow discharges, which is similar to the results observed in the case of sub-centimeter DC glow discharges in ambient air [13].

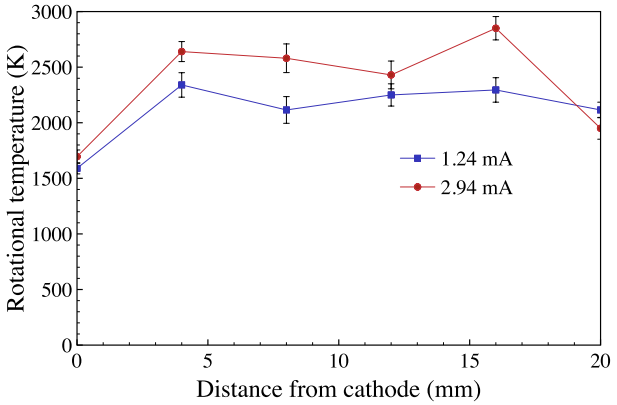

FIGURE 10. Spatially resolved rotational temperatures of subnormal and transitional glow discharges generated between two Cu rod electrodes with 2 cm spacing.

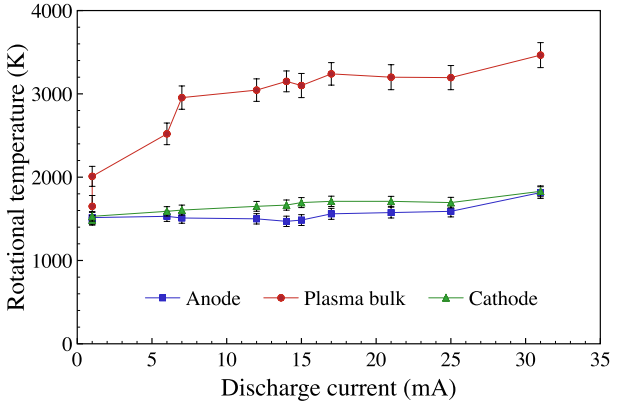

FIGURE 11. Rotational temperature of N_2 as a function of the discharge current for the glow discharge generated between two Cu rod electrodes with 0.5 cm spacing.

In the case of subnormal glow discharge, rotational temperature was about 2300 K in the top and bottom of the positive column, when in the middle of the column, it decreased to about 2100 K — which is in good agreement with the image recorded by the high-speed camera (Figure 8d), where emission in the center of the positive column was weaker compared to the top and bottom areas.

A similar picture was observed for transitional glow discharge, except in the upper area of the positive column. A plot of the rotational temperature is in good agreement with a plot for OH normalized intensity (Figure 9b), which represents the amount of electrons with energies higer than 18.5 eV. Additionally, the spatially resolved rotational temperature of the transitional glow discharge is in good agreement with the high-speed camera image (Figure 8h), where the intensity of the emission was stronger in the upper area of the positive column.

To check the effect of the current on rotational temperature, glow discharge in 0.5 cm gaps could be used due to the absence of discharge fluctuation caused by convection flow and the lower rate of heating of the electrodes. Owing to the lower power required for generation of normal glow discharge in 0.5 cm gaps (Figure 6), it was possible to measure reliable N_2 emission spectra in the area of 380 nm for discharge currents in the range of 0.97 – 31.2 mA, which covers subnormal, transitional, and normal glow discharge areas. Figure 11 shows the rotational temperature of N_2 as a function of the discharge current for the discharge in 0.5 cm gaps in the areas of the cathode, plasma bulk (positive column), and anode.

It could be noted that in 0.5 cm gaps, values of rotational temperatures of the subnormal discharge in the positive column are similar to those in the case of 2 cm gap (about 2000 K for 0.5 cm and 2100 K for 2 cm). Moreover, temperature increases in the case of transitional glow discharge compared to subnormal glow, when temperature in the anode and cathode regions remains low. In the case of 0.5 cm gaps, temperature increases rapidly with transfer to normal glow discharge reaching values of up to 3500 K. Considering the similar behavior of subnormal and transitional glow discharges in 0.5 and 2 cm gaps, it could be considered that in the case of 2 cm gaps, with the increase of discharge current, rotational temperatures for the normal glow regime could reach 3500 K and above, owing to the higher power input.

The observed variation of the rotational temperature in a wide range (from 1650 to 3500 K), which could be controlled by setting parameters of the DC PSU, looks promising for plasma treatment applications in various fields (gas decomposition, radicals production, surface treatment, etc.) where precise control of the gas temperature is required.

G. TWO-STEP GENERATION OF RE-PULSING GLOW DISCHARGE IN 2 cm GAPS

Commonly, glow discharge in molecular gases, such as ambient air, is ignited in sub-centimeter gaps, followed by extention of the gap between the electrodes to the desired length or by using additional generators for ignition of high-frequency discharge followed by generation of glow discharge. In both cases, termination of plasma due to some external factor (e.g., external airflow) leads to problems with reinitiation of the discharge. If plasma was terminated, it will require to manipulate electrodes or use an additional plasma generator for reinitiation of the discharge; therefore, an alternative approach which does not require additional power supply or manipulation of the electrodes is desired. The generator used in the present work looks promising for generation of re-pulsing glow discharge in centimeter-order gaps as a sequence of spark discharge followed by re-pulsing glow discharge, in a similar way as it was reported elsewhere [44]–[46], [55]. In the case of 2 cm gaps between the electrodes, it will require more than 22 kV of voltage applied to the electrodes for generation of spark discharge

to initiate re-pulsing glow discharge in the afterglow of the spark. Voltage on the output of the generator depends on the voltage set on the DC PSU, which powers the push–pull generator; therefore, the voltage on the DC PSU should be set to a value which ensures generation of more than 22 kV on the secondary winding. For that reason, the voltage on the DC PSU was limited by 30 V (enough to produce 25 kV on secondary winding) and the amount of power supplied to the push–pull generator was controlled by limiting the current supplied by the DC PSU. By limiting the current, it was possible to generate all three types of discharges (corona, repeating spark, re-pulsing glow) discussed in chapter 3.A. However, in the case of direct application of current sufficient for sustaining glow discharge (above 3 A DC current supplied to the push–pull generator), discharge happens as a sequence of corona, spark, and re-pulsing glow discharge. Current and voltage waveforms of the discharge generated by turning on the DC PSU with a current limited by 5 A (which is sufficient for generation of transitional glow) and voltage limited by 30 V (sufficient for providing more than the 22 kV required for breakdown of the discharge gap) are presented in Figure 12.

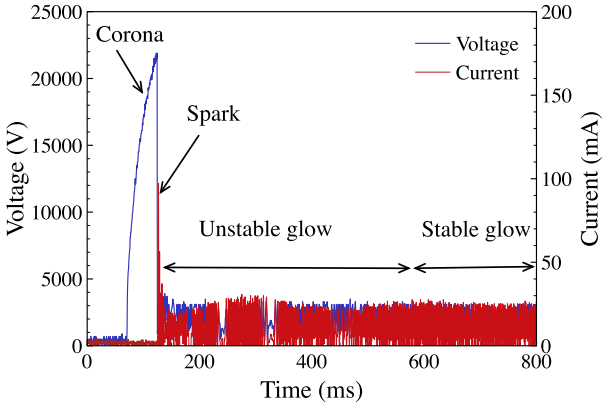

FIGURE 12. Current and voltage waveforms of re-pulsing glow discharge generated by the transition from the spark in 2 cm gap.

The DC PSU was turned on at about 80 ms (Figure 12) and started to charge the capacitor, resulting in an increase of voltage. When the voltage reached about 22.5 kV, the spark discharge happened (150 ms, Figure 12) and was followed immediately by re-pulsing glow. After initiation, glow discharge fluctuated for some time (period from spark discharge to 600 ms, Figure 12) and stabilized after. In the case of transitional glow, the time after initiation of the discharge required for stabilization was about 0.5 s and it reduced with an increase of the discharge current (0.2–0.3 s for normal glow). On the other hand, in the case of subnormal glow, stabilization required a few seconds (1–5 s), and at low currents required several spark discharges prior to the generation of re-pulsing glow.

An advantage of proposed approach is that glow discharge could be generated in centimeter-order gaps with defined parameters (limiting the current and voltage of the DC PSU prior to the discharge), using a single generator without manipulation of electrodes, by just turning on the DC PSU. Moreover, if discharge is terminated by any external factor, it will just restart automatically as a sequence of spark and glow discharge, which looks promising for practical applications. A compact device which does not require any pre-ignition or manipulation of electrodes could be used for energy efficient processing, due to the possibility to define discharge parameters and gas temperature before the discharge, which eliminates power losses diring tuning of plasma parameters before plasma treatment.

H. APPLICABILITY OF RE-PULSING GLOW DISCHARGE TO TREATMENT OF THE GAS FLOW

The relatively high temperature produced by glow discharge results in the formation of a temperature gradient and strong convection flow of the gas. If the electrodes in the present system are placed horizontally, discharge will be elongated by upstream convection flow. Figure 13 illustrates images of the horizontal elongated subnormal and normal glow discharges generated in 1.5 cm gaps.

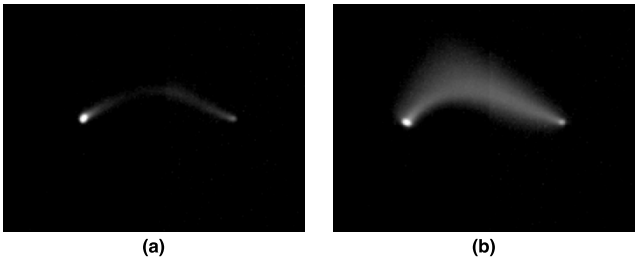

FIGURE 13. Images of horizontal subnormal (a) and normal (b) discharges generated with 1.5 cm electrode spacing recorded using the same exposure time.

Despite elongation of the discharge caused by the convection flow, discharge stabilizes after a few seconds and remains stable for a long time in the same shape. Current and voltage waveforms of the discharge also remain the same, with some insignificant fluctuations. The observed effect confirms that it is possible to achieve stable plasma conditions, even in the case that gas flows through the discharge gap. In the case of precise tuning of gas flow and parameters set for the DC PSU, it is possible to achieve stable glow discharges with the desired parameters, similar to that discussed for the vertical glow discharge system. The reported results suggest that the developed device could be used as an energy efficient analog to the commonly used gliding glow discharge systems. Additionally, considering the low cost of the device and the small number of parts, treatment of gases by re-pulsing glow could be easily scaled by an increase of the number of discharges. However, further investigation of the discharge uniformity and range of stable parameters needs to be conducted for application in the treatment of flowing gases.

IV. CONCLUSION

Re-pulsing glow discharges in centimeter-order gaps were experimentally investigated in atmospheric pressure ambient air. Discharge was ignited as a sequence of spark and glow discharge, and sustained in a glow regime after ignition. It was confirmed that discharge with defined parameters could be ignited without any adjustments after initiation of the discharge.

The discharges were characterized by a high-speed camera, current and voltage measurements, and optical emission spectrometry (OES). The typical structure of the glow discharge consisting of cathode glow, dark Faraday space, positive column, and anode glow was observed. Transition from subnormal to normal glow was confirmed by analysis of average discharge voltage as a function of average discharge current. It was found by OES that the type of discharge strongly affects the ratio of the produced reactive species. In subnormal glow, mostly N_2 second positive emission was observed, when in the case of normal glow discharge, OH emission lines were dominant. It was confirmed that with the change of discharge from subnormal to normal glow regime, rotational temperature could vary across a wide range (from 1650 to 3500 K), which could be useful in practical applications.

The developed device allows to ignite glow discharge with defined parameters, which makes possible the control of the gas temperature and ratio of reactive species by presetting the discharge parameters. Additionally, the possibility of treatment of flowing gas was demonstrated.

Further investigations concerning the non-uniformity of the positive column in the case of longer gaps and effect of the gas flow on plasma parameters are desired for uniform treatment of gases or other targets by plasma using the reported device.

REFERENCES

[1] N. Saito, M. A. Bratescu, and K. Hashimi, "Solution plasma: A new reaction field for nanomaterials synthesis," *Jpn. J. Appl. Phys.*, vol. 57, no. 1, Jan. 2018, Art. no. 0102A4.

[2] J. Winter, R. Brandenburg, and K.-D. Weltmann, "Atmospheric pressure plasma jets: An overview of devices and new directions," *Plasma Sources Sci. Technol.*, vol. 24, no. 6, 2015, Art. no. 064001.

[3] S. Bekeschus, A. Schmidt, K.-D. Weltmann, and T. von Woedtke, "The plasma jet kINPen—A powerful tool for wound healing," *Clin. Plasma Med.*, vol. 4, no. 1, pp. 19–28, Jul. 2016.

[4] P. Bruggeman *et al.*, "Plasma-liquid interactions: A review and roadmap," *Plasma Sources Sci. Technol.*, vol. 25, no. 5, Sep. 2016, Art. no. 053002.

[5] E. Y. Gusev, O. A. Ageev, V. A. Gamaleev, A. S. Mikhno, O. O. Mironenko, and E. A. Pronin, "Effect of annealing on conductivity type of nanocrystalline ZnO films fabricated by RF magnetron sputtering," *Adv. Mater. Res.*, vol. 893, pp. 539–542, Feb. 2014.

[6] M. Ito, J.-S. Oh, T. Ohta, M. Shiratani, and M. Hori, "Current status and future prospects of agricultural applications using atmospheric-pressure plasma technologies," *Plasma Process. Polym.*, vol. 15, no. 2, Feb. 2018, Art. no. 1700073.

[7] J. Zhang, T. Kwon, S. Kim, and D. Jeong, "Plasma farming: Non-thermal dielectric barrier discharge plasma technology for improving the growth of soybean sprouts and chickens," *Plasma*, vol. 1, no. 2, pp. 285–296, 2018.

[8] N. Puač, M. Gherardi, and M. Shiratani, "Plasma agriculture: A rapidly emerging field," *Plasma Process. Polym.*, vol. 15, no. 2, Feb. 2018, Art. no. 1700174.

[9] I. Schweigert, D. Zakrevsky, P. Gugin, E. Yelak, E. Golubitskaya, O. Troitskaya, and O. Koval, "Interaction of cold atmospheric argon and helium plasma jets with bio-target with grounded substrate beneath," *Appl. Sci.*, vol. 9, no. 21, p. 4528, 2019.

[10] S. Ito, K. Sakai, V. Gamaleev, M. Ito, M. Hori, M. Kato, and M. Shimizu, "Oxygen radical based on non-thermal atmospheric pressure plasma alleviates lignin-derived phenolic toxicity in yeast," *Biotechnol. Biofuels*, vol. 13, no. 1, p. 18, Dec. 2020.

[11] F. Rezaei, Y. Gorbanev, M. Chys, A. Nikiforov, S. W. H. Van Hulle, P. Cos, A. Bogaerts, and N. De Geyter, "Investigation of plasma-induced chemistry in organic solutions for enhanced electrospun PLA nanofibers," *Plasma Process. Polym.*, vol. 15, no. 6, Jun. 2018, Art. no. 1700226.

[12] R. H. Stark and K. H. Schoenbach, "Direct current glow discharges in atmospheric air," *Appl. Phys. Lett.*, vol. 74, no. 25, pp. 3770–3772, Jun. 1999.

[13] P. Bruggeman, J. Liu, J. Degroote, M. G. Kong, J. Vierendeels, and C. Leys, "DC excited glow discharges in atmospheric pressure air in pin-to-water electrode systems," *J. Phys. D, Appl. Phys.*, vol. 41, no. 21, Nov. 2008, Art. no. 215201.

[14] D. Staack, B. Farouk, A. Gutsol, and A. Fridman, "Characterization of a DC atmospheric pressure normal glow discharge," *Plasma Sources Sci. Technol.*, vol. 14, no. 4, pp. 700–711, Nov. 2005.

[15] D. Staack, B. Farouk, A. F. Gutsol, and A. A. Fridman, "Spectroscopic studies and rotational and vibrational temperature measurements of atmospheric pressure normal glow plasma discharges in air," *Plasma Sources Sci. Technol.*, vol. 15, no. 4, pp. 818–827, Nov. 2006.

[16] X. Li, P. Zhang, P. Jia, J. Chu, and J. Chen, "Generation of a planar direct-current glow discharge in atmospheric pressure air using rod array electrode," *Sci. Rep.*, vol. 7, no. 1, Dec. 2017, Art. no. 2672.

[17] V. I. Arkhipenko, A. A. Kirillov, Y. A. Safronau, and L. V. Simonchik, "DC atmospheric pressure glow microdischarges in the current range from microamps up to amperes," *Eur. Phys. J. D*, vol. 60, no. 3, pp. 455–463, Dec. 2010.

[18] D. Staack, B. Farouk, A. Gutsol, and A. Fridman, "DC normal glow discharges in atmospheric pressure atomic and molecular gases," *Plasma Sources Sci. Technol.*, vol. 17, no. 2, May 2008, Art. no. 025013.

[19] K. Miyamoto, S. Ikehara, H. Takei, Y. Akimoto, H. Sakakita, K. Ishikawa, M. Ueda, J.-I. Ikeda, M. Yamagishi, J. Kim, T. Yamaguchi, H. Nakanishi, T. Shimizu, N. Shimizu, M. Hori, and Y. Ikehara, "Red blood cell coagulation induced by low-temperature plasma treatment," *Arch. Biochem. Biophys.*, vol. 605, pp. 95–101, Sep. 2016.

[20] D. Y. Kim, S. J. Kim, H. M. Joh, and T. H. Chung, "Characterization of an atmospheric pressure plasma jet array and its application to cancer cell treatment using plasma activated medium," *Phys. Plasmas*, vol. 25, no. 7, Jul. 2018, Art. no. 073505.

[21] J.-S. Oh, E. J. Szili, K. Ogawa, R. D. Short, M. Ito, H. Furuta, and A. Hatta, "UV–vis spectroscopy study of plasma-activated water: Dependence of the chemical composition on plasma exposure time and treatment distance," *Jpn. J. Appl. Phys.*, vol. 57, no. 1, Jan. 2018, Art. no. 0102B9.

[22] Z. Machala, B. Tarabová, D. Sersenová, M. Janda, and K. Hensel, "Chemical and antibacterial effects of plasma activated water: Correlation with gaseous and aqueous reactive oxygen and nitrogen species, plasma sources and air flow conditions," *J. Phys. D, Appl. Phys.*, vol. 52, no. 3, Jan. 2019, Art. no. 034002.

[23] A. Khlyustova, C. Labay, Z. Machala, M.-P. Ginebra, and C. Canal, "Important parameters in plasma jets for the production of RONS in liquids for plasma medicine: A brief review," *Frontiers Chem. Sci. Eng.*, vol. 13, no. 2, pp. 238–252, Jun. 2019.

[24] H. Xu, D. Liu, W. Wang, Z. Liu, L. Guo, M. Rong, and M. G. Kong, "Investigation on the RONS and bactericidal effects induced by He + O_2 cold plasma jets: In open air and in an airtight chamber," *Phys. Plasmas*, vol. 25, no. 11, Nov. 2018, Art. no. 113506.

[25] V. Gamaleev, N. Iwata, M. Hori, M. Hiramatsu, and M. Ito, "Direct treatment of liquids using low-current arc in ambient air for biomedical applications," *Appl. Sci.*, vol. 9, no. 17, p. 3505, 2019.

[26] N. Iwata, V. Gamaleev, J. Oh, T. Ohta, M. Hori, and M. Ito, "Investigation on the long-term bactericidal effect and chemical composition of radical-activated water," *Plasma Process. Polym.*, vol. 16, no. 10, Oct. 2019, Art. no. 1900055.

[27] V. Gamaleev, N. Iwata, J.-S. Oh, M. Hiramatsu, and M. Ito, "Development of an ambient air flow rotating arc jet for low-temperature treatment," *IEEE Access*, vol. 7, pp. 93100–93107, 2019.

[28] J.-S. Oh, M. Kakuta, H. Furuta, H. Akatsuka, and A. Hatta, "Effect of plasma jet diameter on the efficiency of reactive oxygen and nitrogen species generation in water," *Jpn. J. Appl. Phys.*, vol. 55, no. 6S2, Jun. 2016, Art. no. 06HD01.
[29] Y. D. Korolev, O. B. Frants, N. V. Landl, and A. I. Suslov, "Low-current plasmatron as a source of nitrogen oxide molecules," *IEEE Trans. Plasma Sci.*, vol. 40, no. 11, pp. 2837–2842, Nov. 2012.
[30] E. Stoffels, Y. A. Gonzalvo, T. D. Whitmore, D. L. Seymour, and J. A. Rees, "Mass spectrometric detection of short-living radicals produced by a plasma needle," *Plasma Sources Sci. Technol.*, vol. 16, no. 3, pp. 549–556, Aug. 2007.
[31] E. Stoffels, Y. A. Gonzalvo, T. D. Whitmore, D. L. Seymour, and J. A. Rees, "A plasma needle generates nitric oxide," *Plasma Sources Sci. Technol.*, vol. 15, no. 3, pp. 501–506, Aug. 2006.
[32] V. Gamaleev, N. Iwata, M. Hiramatsu, and M. Ito, "Tuning of operational parameters for effective production of nitric oxide using an ambient air rotating glow discharge jet," *Jpn. J. Appl. Phys.*, vol. 59, May 2020, Art. no. SHHF04.
[33] R. H. Stark and K. H. Schoenbach, "Direct current high-pressure glow discharges," *J. Appl. Phys.*, vol. 85, no. 4, pp. 2075–2080, Feb. 1999.
[34] O. Mutaf-Yardimci, A. V. Saveliev, A. A. Fridman, and L. A. Kennedy, "Thermal and nonthermal regimes of gliding arc discharge in air flow," *J. Appl. Phys.*, vol. 87, no. 4, pp. 1632–1641, Feb. 2000.
[35] J. Pawłat, P. Terebun, M. Kwiatkowski, B. Tarabová, Z. Kovalová, K. Kučerová, Z. Machala, M. Janda, and K. Hensel, "Evaluation of oxidative species in gaseous and liquid phase generated by mini-gliding arc discharge," *Plasma Chem. Plasma Process.*, vol. 39, no. 3, pp. 627–642, May 2019.
[36] Y. D. Korolev, O. B. Frants, N. V. Landl, A. V. Bolotov, and V. O. Nekhoroshev, "Features of a near-cathode region in a gliding arc discharge in air flow," *Plasma Sources Sci. Technol.*, vol. 23, no. 5, 2014, Art. no. 054016.
[37] Y. D. Korolev, O. B. Frants, V. G. Geyman, N. V. Landl, and V. S. Kasyanov, "Low-current 'gliding arc' in an air flow," *IEEE Trans. Plasma Sci.*, vol. 39, no. 12, pp. 3319–3325, Dec. 2011.
[38] V. Gamaleev, N. Iwata, G. Ito, M. Hori, M. Hiramatsu, and M. Ito, "Scalable treatment of flowing organic liquids using ambient-air glow discharge for agricultural applications," *Appl. Sci.*, vol. 10, no. 3, p. 801, 2020.
[39] S. Gröger, M. Ramakers, M. Hamme, J. A. Medrano, N. Bibinov, F. Gallucci, A. Bogaerts, and P. Awakowicz, "Characterization of a nitrogen gliding arc plasmatron using optical emission spectroscopy and high-speed camera," *J. Phys. D, Appl. Phys.*, vol. 52, no. 6, Feb. 2019, Art. no. 065201.
[40] H. Zhang, L. Li, X. Li, W. Wang, J. Yan, and X. Tu, "Warm plasma activation of CO_2 in a rotating gliding arc discharge reactor," *J. CO_2 Utilization*, vol. 27, pp. 472–479, Oct. 2018.
[41] R. L. Bright, G. F. Pittman, and G. M. Royer, "Transistors as on-off switches in saturable core circuits," *Elect. Manuf.*, vol. 54, pp. 79–82, Dec. 1954.
[42] J. Williams, *The Art and Science of Analog Circuit Design*. Boston, MA, USA: Butterworth-Heinemann, 1998.
[43] V. F. Tarasenko, E. K. Baksht, I. D. Kostyrya, and V. Shutko, "Runaway electron preionized diffuse discharges in atmospheric pressure air with a point-to-plane gap in repetitive pulsed mode," *J. Appl. Phys.*, vol. 109, no. 8, Apr. 2011, Art. no. 083306.
[44] Z. Machala, I. Jedlovsky, and V. Martisovits, "DC discharges in atmospheric air and their transitions," *IEEE Trans. Plasma Sci.*, vol. 36, no. 4, pp. 918–919, Aug. 2008.
[45] Y. Akishev, M. Grushin, I. Kochetov, V. Karal'nik, A. Napartovich, and N. Trushkin, "Negative corona, glow and spark discharges in ambient air and transitions between them," *Plasma Sources Sci. Technol.*, vol. 14, no. 2, pp. S18–S25, May 2005.
[46] Y. Akishev, M. Grushin, V. Karalnik, A. Petryakov, and N. Trushkin, "Non-equilibrium constricted DC glow discharge in N2flow at atmospheric pressure: Stable and unstable regimes," *J. Phys. D, Appl. Phys.*, vol. 43, no. 7, Feb. 2010, Art. no. 075202.
[47] M. R. Webb, F. J. Andrade, G. Gamez, R. McCrindle, and G. M. Hieftje, "Spectroscopic and electrical studies of a solution-cathode glow discharge," *J. Anal. At. Spectrometry*, vol. 20, no. 11, pp. 1218–1225, 2005.
[48] V. Gamaleev, H. Furuta, and A. Hatta, "Generation of micro-arc discharge plasma in highly pressurized seawater," *Appl. Phys. Lett.*, vol. 113, no. 21, Nov. 2018, Art. no. 214102.
[49] Y. P. Raizer, *Gas Discharge Physics*, 1st ed. Berlin, Germany: Springer-Verlag, 1991.
[50] P. J. Bruggeman, N. Sadeghi, D. C. Schram, and V. Linss, "Gas temperature determination from rotational lines in non-equilibrium plasmas: A review," *Plasma Sources Sci. Technol.*, vol. 23, no. 2, 2014, Art. no. 023001.
[51] W. Jiang, J. Tang, Y. Wang, W. Zhao, and Y. Duan, "Characterization of argon direct-current glow discharge with a longitudinal electric field applied at ambient air," *Sci. Rep.*, vol. 4, no. 1, May 2015, Art. no. 6323.
[52] G. Herzberg, *Molecular Spectra and Molecular Structure: Spectra of Diatomic Molecules*, vol. 1, 2nd ed. Toronto, ON, Canada: D. Van Mostrand Company, 1950.
[53] T.-L. Zhao, Y. Xu, Y.-H. Song, X.-S. Li, J.-L. Liu, J.-B. Liu, and A.-M. Zhu, "Determination of vibrational and rotational temperatures in a gliding arc discharge by using overlapped molecular emission spectra," *J. Phys. D, Appl. Phys.*, vol. 46, no. 34, Aug. 2013, Art. no. 345201.
[54] N. Britun, M. Gaillard, S.-G. Oh, and J. G. Han, "Fabry–Perot interferometry for magnetron plasma temperature diagnostics," *J. Phys. D, Appl. Phys.*, vol. 40, no. 17, pp. 5098–5108, Sep. 2007.
[55] V. F. Tarasenko, E. A. Sosnin, V. S. Skakun, V. A. Panarin, M. V. Trigub, and G. S. Evtushenko, "Dynamics of apokamp-type atmospheric pressure plasma jets initiated in air by a repetitive pulsed discharge," *Phys. Plasmas*, vol. 24, no. 4, Apr. 2017, Art. no. 043514.

VLADISLAV GAMALEEV received the M.Sc. degree from Southern Federal University, Russia, in 2011, and the Ph.D. (Eng.) degree from the Kochi University of Technology, Japan, in 2018. He is currently a Postdoctoral Researcher with Nagoya University. His research interests include plasma generation at atmospheric and high pressure in gas and liquid phase, and plasma diagnostics. He is currently focusing on biomedical and agricultural applications of atmospheric pressure plasmas. He is a member of the Japan Society of Applied Physics (JSAP).

TAKAYOSHI TSUTSUMI received the Ph.D. degree from the Division of Engineering, Graduate School, Nagoya University, Japan, in 2015. In 2015, he joined Nagoya University, where he is currently an Assistant Professor.

MINEO HIRAMATSU received the M.Eng. and Ph.D. (Eng.) degrees from Nagoya University. He is currently a Full Professor with the Department of Electrical and Electronic Engineering, Meijo University, Japan. He also serves as the Director of the Research Institute, Meijo University. He is author of more than 150 scientific articles and patents on plasma processes for materials science, author of five books, and more than 30 invitations to speak at international conferences on plasma science and nanomaterials. His main fields of research are plasma diagnostics and plasma processing for the synthesis of thin films and nanostructured materials. He is a Fellow of the Japan Society of Applied Physics.

MASAFUMI ITO (Member, IEEE) received the B.Sc. (Eng.), M.Eng., and Ph.D. (Eng.) degrees from Nagoya University, Aichi, Japan, in 1986, 1988, and 1992, respectively. He was a Research Associate and then an Assistant Professor with Nagoya University, from 1991 to 1999. He was an Associate Professor and then a Professor with Wakayama University, from 1999 to 2009. Since 2009, he has been a Professor with Meijo University, Japan. Since 2014, he has been the Director of the Research Center of Plasma-Bio Science and Technology, Meijo University. He is currently with Meijo University. His current research interests include plasma science, and applications for agriculture and life science.

MASARU HORI (Member, IEEE) received the B.E. and M.E. degrees from Waseda University, Tokyo, Japan, in 1981 and 1983, respectively, and the D.E. degree from Nagoya University, Nagoya, Japan, in 1986. He was a Researcher with Toshiba Corporation, from 1986 to 1992. He was a Research Associate, an Assistant Professor, and then an Associate Professor with Nagoya University, from 1992 to 2004. Since 2004, he has been a Professor with Nagoya University. He was the Director of the Plasma Nano Research Center, from 2009 to 2013. He was the Director of the Plasma Medical Science Global Innovation Center, Nagoya University, from 2013 to 2019. Since 2019, he has been the Director of the Center for Low-Temperature Plasma Science, Nagoya University. He is currently with Nagoya University. His current research interests include plasma nano-processing and life sciences.